JOURNAL OF MATERIALS SCIENCE 26 (1991) 4751–4758

Mechanical behaviour of a cross-weave ceramic matrix composite

Part I *Tensile and compressive loading*

Z. G. WANG†, C. LAIRD, Z. HASHIN‡
School of Engineering and Applied Science, University of Pennsylvania, Philadelphia, PA 19104, USA

B. W. ROSEN, CHIAN-FONG YEN
Materials Sciences Corporation, Gwynedd Plaza II, Bethlehem Pike, Spring House, PA 19477, USA

The deformation and fracture processes of a cross-weave carbon fibre/SiC composite prepared by a chemical vapour deposition process has been explored by interrupted-loading tests and SEM examination of cracking and fracture processes. The tensile stress–strain curves show non-linear behaviour associated with progressive matrix cracking and spalling, and the occasional fracture of a fibre. Re-loading curves and compressive stress–strain curves show linear behaviour. The fracture process does not involve cracking by a single dominant crack but occurs by the development of multiple damage sites operating around the transverse fractures of groups of four to eight fibres followed by longitudinal cracking at their fibre–matrix interfaces and temporary arrest of the cracks, until specimen failure occurs and there is massive fibre debonding and pull-out.

1. Introduction

Both continuous and discontinuous fibre-reinforced ceramic matrix composites have recently received a great deal of attention [1–3]. The primary reason for these accelerated efforts lies in the assumption that strong ceramic fibres can prevent catastrophic brittle failure in ceramics by providing various energy dissipation processes during a crack advance (if that, indeed, is the failure mechanism). Strong ceramic fibres can also be used as reinforcing elements in a metal matrix. However, the philosophy of designing is quite different between metal matrix and ceramic matrix composites. In metal matrix composites, fibres are added to increase both the elastic modulus and the strength of the metallic matrix at the expense of its fracture toughness. The well-known aluminium alloy matrix composites provide such an example. In ceramic matrix composites, the fibres are added with the aim of increasing the fracture toughness of the ceramic matrix without necessarily improving the elastic properties. Thus the strong fibres are used to obtain a good combination of strength and toughness.

The development of ceramic matrix composites began with carbon fibre-reinforced glasses almost 20 years ago [4, 5]. However, these composites are vulnerable to degradation in an oxidizing environment at relatively low temperatures. Since continuous-polymer-derived SiC fibres (Nicalon), which are more oxidation resistant than carbon fibres and are chemically compatible with many ceramic matrices, became commercially available by the end of the '70s, very close attention has been given to the development of ceramic composites reinforced with Nicalon and other ceramic fibres. The newly developed ceramic matrix composites are very different from the existing composites, such as carbon–carbon or metal matrix composites reinforced with ceramics and can be loosely grouped into two categories: fibre-dominated composites and matrix-dominated composites. The fibre dominated composites use a glass matrix the modulus of which is much lower than that of the fibres. Because the fibres are so much stiffer, they carry the largest proportion of the load and therefore the stiffness and strength of the composite are governed to a large extent by the fibre properties. In this respect, the glass matrix composites are similar to existing organic, carbon and metal matrix composites. In matrix-dominated composites, the matrix can be as stiff as the fibres, and possibly even stiffer than the fibres. Therefore, the matrix will carry a large portion of the load and contributes substantially to the compliance, strength and toughness of the composite. The major role of the fibres appears to be their influence upon the mechanisms of local damage initiation, growth and arrest.

In the past decade, extensive work has been done on

†*Permanent address*: Institute of Metals Research, Academia Sinica, Shenyang, China.
‡*Permanent address*: Tel Aviv University, Israel.

0022–2461/91 $03.00 + .12 © *1991 Chapman & Hall*

the development of glass-ceramic composites which has stimulated considerable advances in understanding mechanical behaviours and failure mechanisms of ceramic composites. It was reported [6, 7] that the fibre-dominated composites have non-linear and irreversible stress–strain response. The knee of the stress–strain curve corresponds to the composite stress level at which the matrix cracks. It is not clear if the matrix dominated composites behave similarly.

The aim of the present experimental study is to determine the mechanical behaviour and possible failure modes operating in a carbon/ceramic composite exposed to both monotonic and cyclic high stress. Knowledge of these factors should improve the accuracy of analysis designed to improve life prediction and material properties by control of composite architecture.

2. Material characterization

The external appearance of the as-supplied composite is shown in Fig. 1. The composite is made up from several layers of carbon fibre bundle cross-weaves, inter-penetrated with SiC particles by a chemical vapour deposition (CVD) process, coated with a layer of SiC, and the whole sintered into a rigid mass. The material was furnished in the specimen configuration shown in Fig. 2 with the carbon plies oriented 0°/90°.

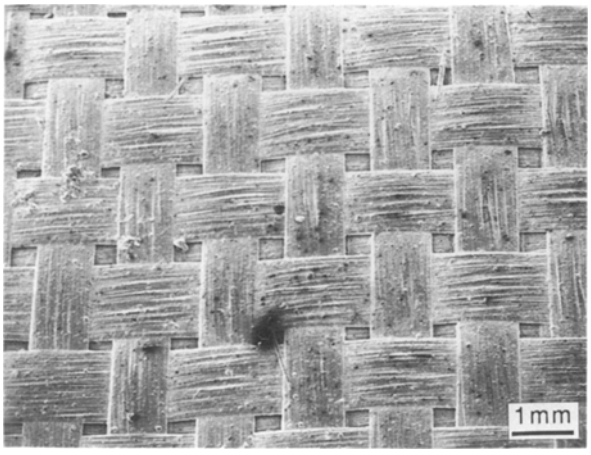

Figure 1 As-received carbon SiC cross-weave composite.

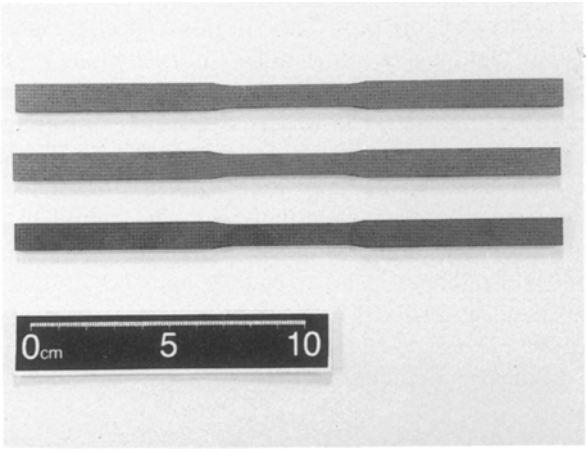

Figure 2 As-received carbon/SiC cross-weave composite specimens.

The distribution of SiC was found to be highly inhomogeneous with a greater thickness existing between plies than between fibres in a bundle, which was reasonably close packed; the external layer of SiC was the thickest. The typical appearance of the intra-bundle regions, viewed by SEM, is shown in Fig. 3. In this particular region, the fibres are not precisely close packed, but contacts between fibres numbering six were commonplace. In the region shown, there are three, four or five contacts per fibre. Fig. 4 shows the Si map obtained by electron diffraction spectroscopy (EDS) corresponding to the region shown in Fig. 3 and this confirms the chemistry of the SiC matrix. Note the highly defective nature of the matrix in which voids were commonplace both at fibre/matrix interfaces and within the matrix. Often these voids were found to be elongated in the fibre direction. The diameters of the fibres typically measured 7–8 μm.

In order to determine the purity of the materials used in the composite and to determine whether or not there was impurity segregation at the fibre/matrix interface, the composite was studied by Auger spectroscopy. Fig. 5 shows a typical fracture surface of the

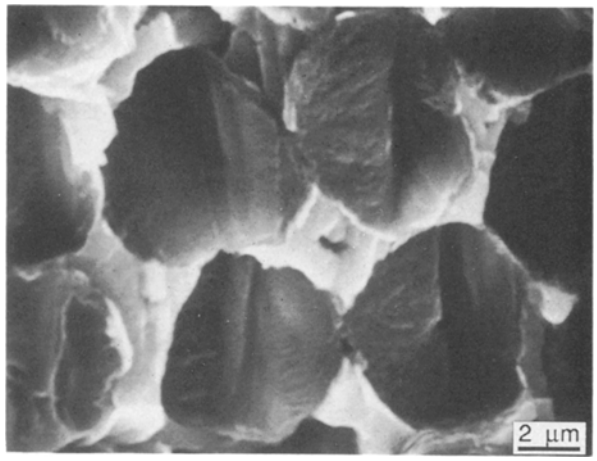

Figure 3 Cross-section through carbon fibre bundle of C/SiC composite, showing deviation from close packing and inhomogeneously distributed SiC matrix. Sectioned by diamond saw.

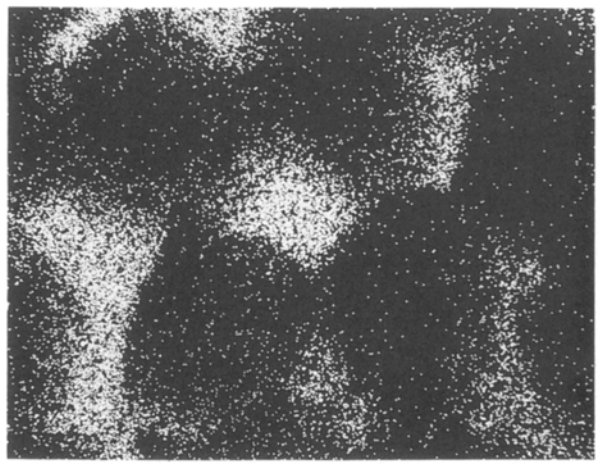

Figure 4 EDAX Si map corresponding to the region shown in Fig. 3, and viewed at the same magnification.

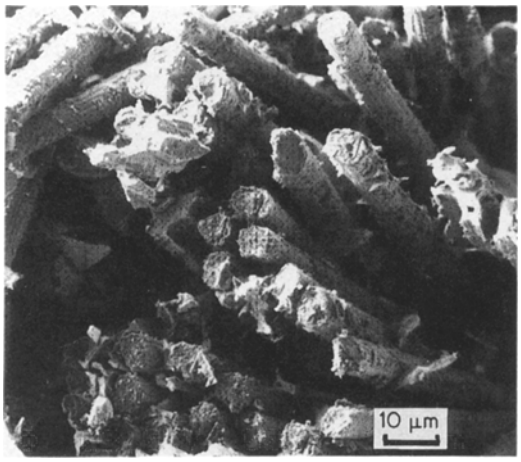

Figure 5 SEM view of composite specimen fractured in the scanning Auger microscope showing the microstructure.

composite broken in the high vacuum of the SAM in order to prevent contamination associated with preparing the sample in air. The fibres were examined both on their fracture surfaces and at the fibre/matrix interfaces revealed by pull-out episodes during the fracture sequence. Plots of the differential of observed Auger intensities against the electron energy are shown in Fig. 6 for both matrix (Fig. 6a) and fibre interface (Fig. 6b), as read on a pulled-out fibre. Only Si and C were detected, the Si level being quite small

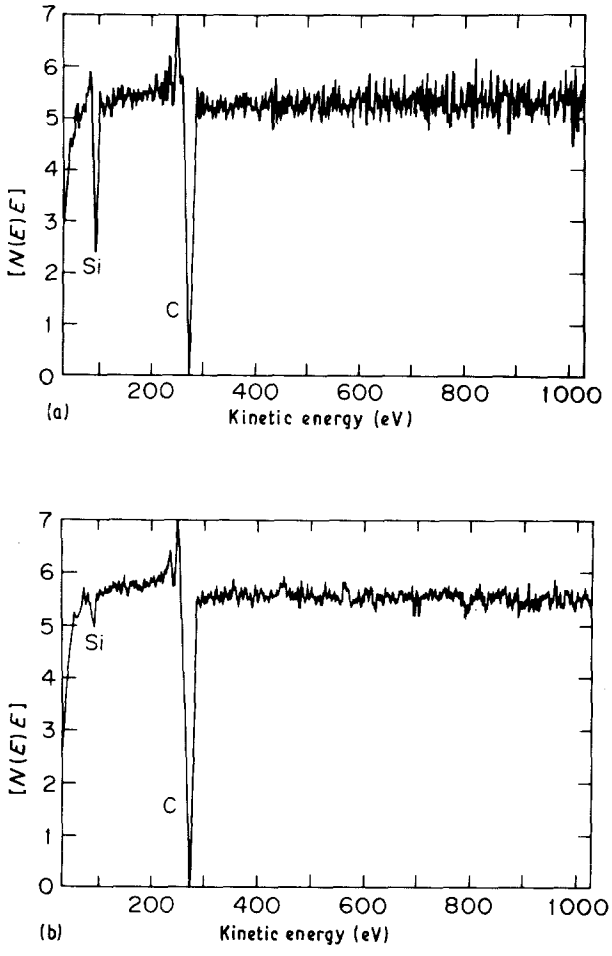

Figure 6 Typical Auger spectra taken from the region shown in Fig. 5: (a) from the matrix; (b) from the fibre/matrix interface.

for the fibre interface. This indicates a small residual adherence of SiC to the fractured interface and apparently no deliberate or accidental modification of the interphase structure.

3. Stress–strain response – monotonic behaviour

3.1. Tensile tests

Tensile tests were carried out with samples of the types shown in Fig. 2 (gauge section measured 3.2 mm × 8.1 mm × 40 mm). Tests were performed in an Instron servo-hydraulic machine, using a clip-on extensometer to measure strain. The tensile strain rate was about $10^{-5}\ s^{-1}$. The specimens were held by friction type grips, and testing alignment was achieved by using universal joints. After the tests were complete, the outer specimen surface and fracture surface were examined by SEM.

A typical stress–strain curve is shown in Fig. 7. It turns out to be similar to the stress–strain curve for SEP Nicalon–SiC composite [8]. The material shows a fairly low elastic limit. The tensile behaviour of the material was found to be highly non-linear and it had a small measure of ductility. The E-modulus (tangent) decreases continuously from about 85 GPa at the beginning of straining to about 36 GPa close to the ultimate stress level. An abrupt load drop occurred at an ultimate strength of about 437 MPa and a corresponding strain of about 1.05%. However, some load-bearing capability was retained beyond the ultimate load, such that further straining proceeded subject to a continuously decreasing stress.

The residual stresses inherited from processing due to differences between the thermal expansion coefficients of the matrix and fibre may have a major effect on the microstresses within a composite material and then play a significant role in the stress–strain behaviour of the composite material. The residual stresses are of course additional to the stresses produced by

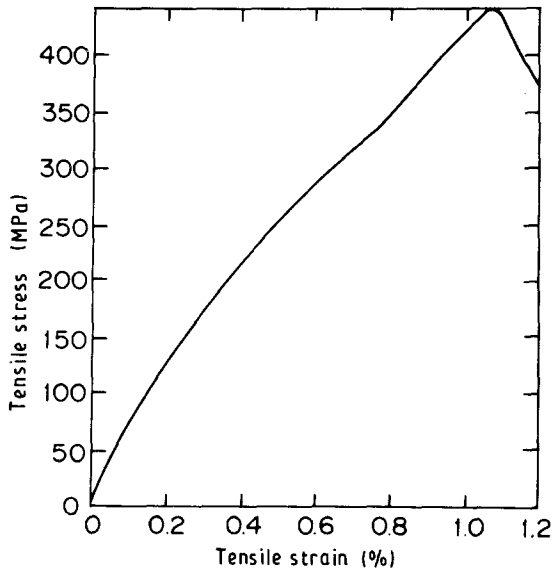

Figure 7 Tensile stress–strain curve for carbon/SiC cross-weave composite. Tested at room temperature.

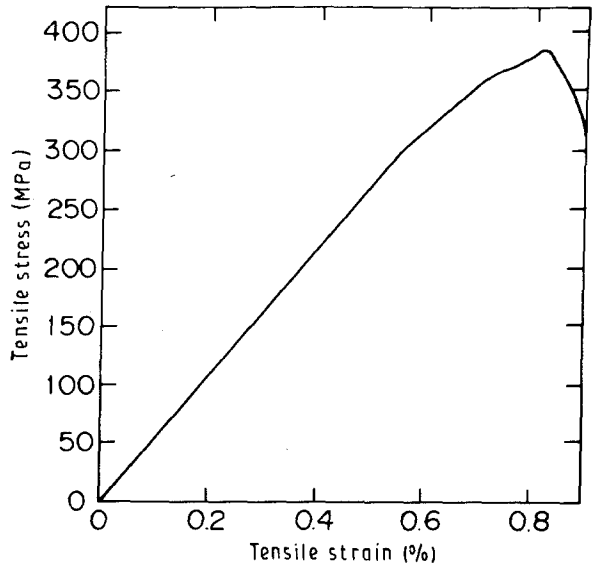

Figure 8 Tensile reloading stress–strain curve of a composite specimen which was initially loaded in tension to a stress of about 306 MPa, and then reloaded.

external loads. Therefore, the residual tensile stresses in the matrix may cause severe microcracking during tensile loading even at a low stress level. Because the matrix is relatively stiff, cracks generating in the matrix and propagating through the composite during tensile loading can be expected to have a large, measurable effect upon the instantaneous composite stiffness. Therefore, it seems reasonable to suggest that the microcracking in the matrix and cracks propagating through the composite are responsible for the continuous reduction of the stiffness. Final failure of fibre bundles and the resulting link-up of multiple cracks in the matrix may be the fundamental processes which dictate the ultimate strength. The region of decreasing stress with increasing strain is associated with fibre pull-out and delamination.

Fig. 8 shows the reloading stress–strain curve of a specimen which was initially loaded to a stress of about 306 MPa, unloaded and then reloaded. Unlike the behaviour shown in Fig. 7 for the as-received specimen, the re-loaded specimen shows a large portion of linear stress–strain behaviour. A deviation from linearity occurred at a stress of about 280 MPa, followed by the usual non-linear region with reduced stiffness. Apparently, the presence of linear behaviour resulted from the fact that numerous matrix microcracks generated in the previous loading exerted their effect on reloading and few new matrix cracks would be generated during tensile reloading until the previous highest stress was exceeded. However, when the reapplied tensile stress increased above 280 MPa, more matrix cracks were created and caused non-linear behaviour, resulting in a large increase in compliance or decrease in stiffness.

3.2. Compressive tests

As indicated above, the stress–strain response of matrix-dominated ceramic composites is mainly governed by the cracks which form internally in the brittle matrix. Therefore, one of the basic problems is to evaluate the stiffness reduction due to such cracks. Many investigations of this kind have been published in the literature but in literally all of them it is assumed that the cracks always remain open. This is a realistic assumption only if the tractions normal to the crack surfaces are tensile. When this traction is compressive, the crack will close and will thus have no effect on stiffness reduction. Compressive tests were performed in this study to verify this argument.

The compressive tests were carried out in a conventional Instron servohydraulic machine. Some of the problems with compressive testing are alignment difficulties, buckling and local crushing of the test specimen. A test fixture which is schematically shown in Fig. 9 was specially designed for the tests. The compressive displacement of the specimen was measured by the attached sensitive extensometer. A typical example of a compressive stress–strain curve for the C/SiC cross-weave composite is shown in Fig. 10. The design of the compression specimen which was cut from the end of the as-received specimen is also shown in Fig. 10 as an insert. The initial non-linear portion of the curve was obviously caused by the two ends of the

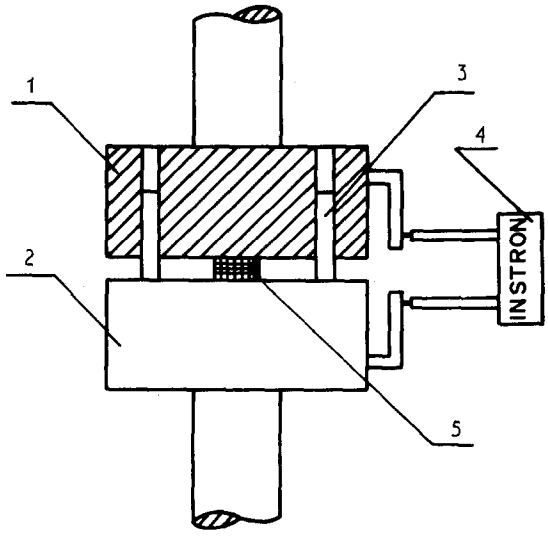

Figure 9 Schematic diagram of the fixture for compressive tests. 1, Upper compressive block; 2, lower compressive block; 3, guide pin; 4, extensometer; 5, specimen.

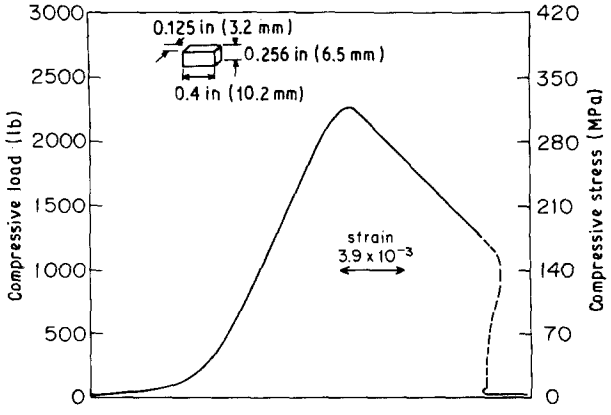

Figure 10 Compressive stress–strain curve at room temperature for carbon/SiC cross-weave composite.

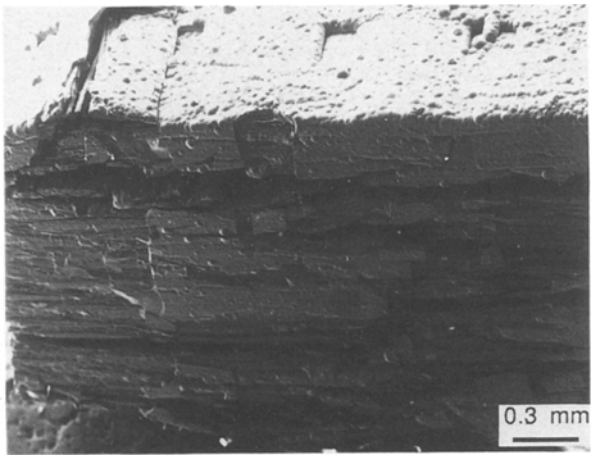

Figure 11 Scanning electron micrograph taken from a specimen which was loaded in compression to the ultimate stress level, showing fibre buckling and matrix fragmentation. The direction of the applied compressive stress is horizontal.

specimen not being precisely parallel. After the initial portion, the compressive stress–strain curve was actually found to be linear up to the ultimate stress level. This behaviour indicated that the growth of existing matrix cracks was suppressed and few new cracks were generated. The ultimate stress level was associated with overall failure, involving particularly the buckling of fibre bundles and matrix fragmentation. A scanning electron micrograph (Fig. 11), recorded immediately after the ultimate load was attained, documented the situation. The continuous decline of load-bearing capacity beyond the ultimate stress reflects the processes of fibre failure, matrix fragmentation and interlayer delamination.

4. Possible fracture processes

It was reported [6] that tensile failure of a unidirectional SiC/glass-ceramic composite included the following sequential processes: the development of a single crack that passes completely through the matrix, but remains bridged by intact fibres, formation of regularly spaced matrix cracks, fibre failure and pull-out. However, the failure mechanism of cross-ply laminates becomes even more complex. Preliminary studies [9] on symmetric (0°/90°) SiC/LAS composite laminates indicated that tensile failure involves several stages of damage development with increasing applied load: edge delamination, matrix cracking in the 90° ply, matrix cracking in the 0° ply, and fibre failure in the 0° ply followed by catastrophic delamination.

In addressing failure processes or local damage mechanisms, it is important to understand the relative roles of both fibre and matrix variability. For short fibres and a large matrix volume, the strength distribution functions of the two constituents are far apart, and extensive matrix cracking without fibre failure is likely. Conversely, for long fibres and small matrix volume, as in the present case, there may be an overlap in the strength distributions of the two phases. It is this latter case which motivates consideration of the early stages of damage growth. It will be appropriate to address matrix microcracking which may be followed by any of the following types of damage: fibre debonding, fibre fracture, matrix crack propagation past unbroken fibres, and the formation of multiple microcracks.

A notched specimen, small enough to fit easily into the SEM sample chamber, was used for studying the sequential failure processes in tension. Fig. 12 shows a typical load versus crosshead displacement curve for such a specimen tested in tension. The configuration of the specimen is also shown in Fig. 12. The appearance of the central part of a specimen before testing is shown in Fig. 13, from which the edge damage by machining can be clearly seen. The specimen was first stretched to 2681 N (600 lb) (just above the knee of the tensile load–deflection curve, see Fig. 12). The resulting damage was observed in the SEM and is shown in Fig. 14. Notice that surface cracks are visible (Fig. 14a) and a single surface crack stretches right to the specimen edge, stimulating local fracture of fibres (Fig. 14b). The specimen was then reloaded, first to 4022 N (900 lb) and again to 4469 N (1000 lb). The

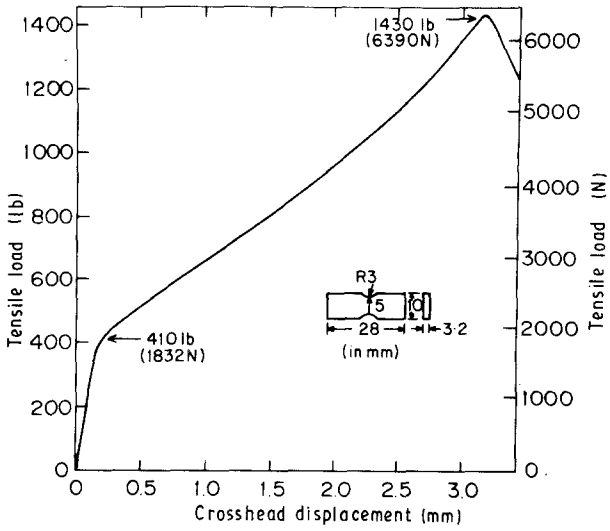

Figure 12 Tensile load versus crosshead displacement curve for a notched composite specimen. Tested at room temperature.

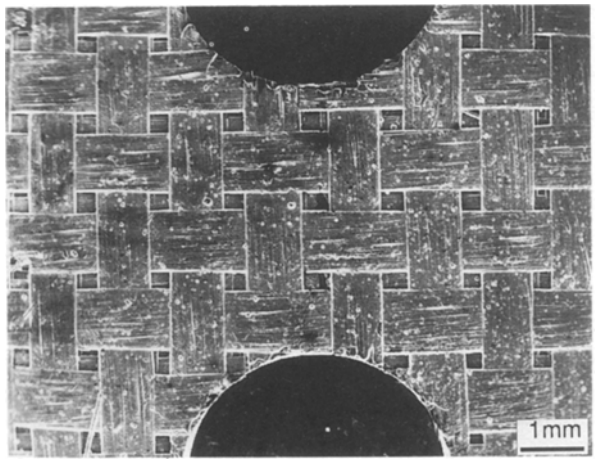

Figure 13 The appearance of the notched gauge section on a specimen for studying tensile failure processes, before loading.

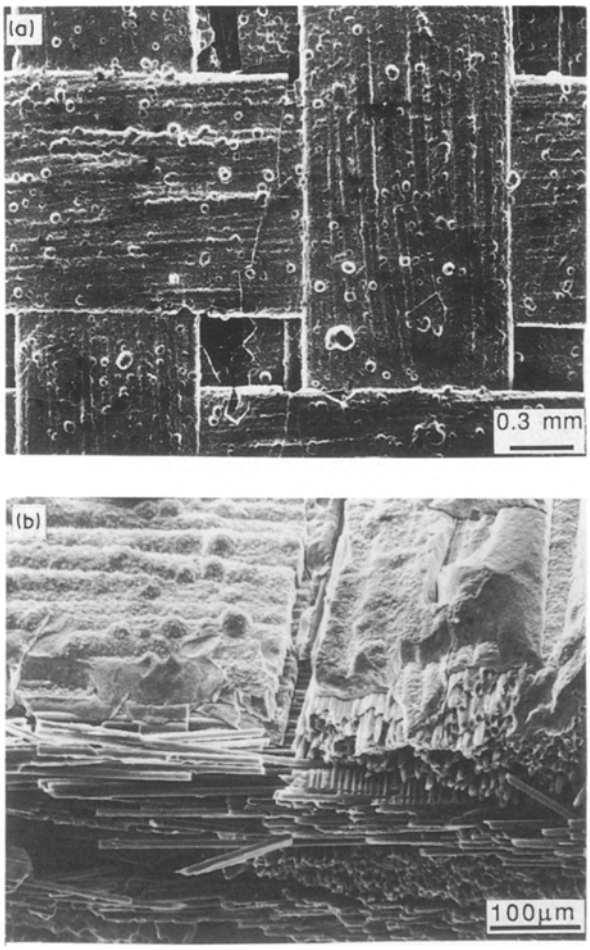

Figure 14 Cracking of C/SiC composite after exposure to tensile load of 2681 N. (a) Normal view, (b) side view.

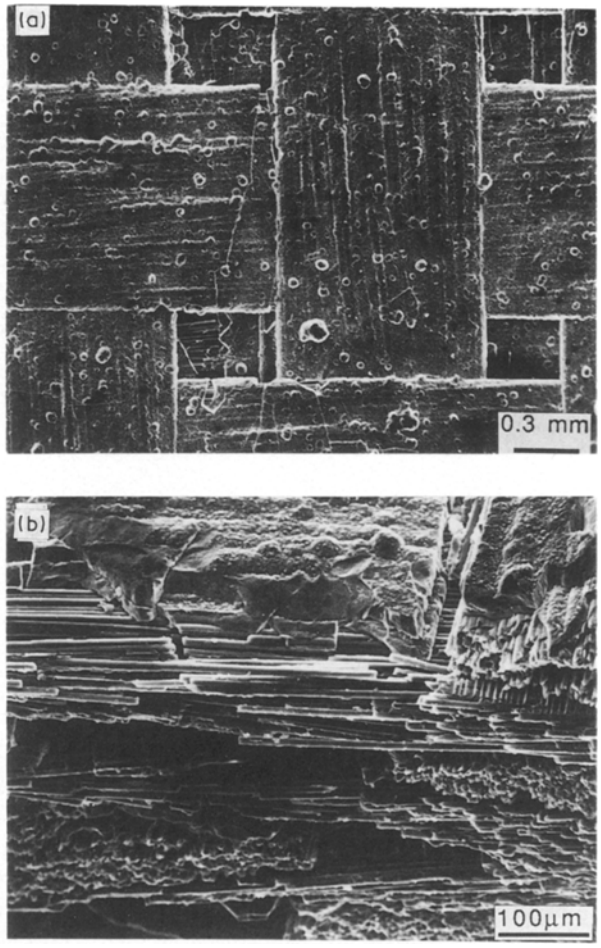

Figure 15 The same area as that shown in Fig. 14 after loading in tension to 4469 N (1000 lb).

same areas were examined by SEM after each reloading. Fig. 15, showing scanning electron micrographs, indicates little subsequent change in surface cracking and spalling even after loading to 4469 N (1000 lb). The specimen was finally fractured at 6256 N. Fig. 16 illustrates the appearance of the fractured specimen at both the top and side of the gauge section. In comparison with the surface cracks shown in Figs 14 and 15, it is clearly seen that the final failure path lies exactly along the surface cracks observed early in the deformation process. Fig. 16 also demonstrates the possible internal damage modes: fibre fracture, delamination and fibre pull-out. It should be noted that the damage appeared more localized than normally observed for long specimens, reflecting the "notched" gauge section of the short specimen used.

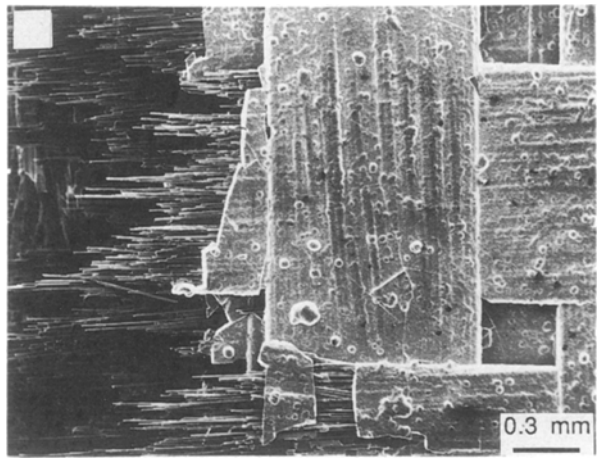

Figure 16 The appearance of the specimen after fracture at 6256 N (1400 lb); the same area as in Figs 14 and 15 is shown.

5. Characteristics of the fracture surface

As indicated above, the tensile failure of a cross-weave C/SiC composite involves several damage modes which are governed by the fibre bundle and matrix variability. One of the most important sources of information relating to the case of failure is the fracture surface itself. A fracture surface shows a detailed record of the failure history of the specimen (which may be too complex to interpret confidently). The principal technique used to analyse fracture surfaces is electron fractography. Fundamental to the application of this technique is an understanding of how materials fracture and how the microstructure (for example, in composites, the constituents and their arrangements) affects the fracture process. Extensive fractographic studies were performed by scanning electron microscopy in the present work.

A macroscopic view of the fracture surface of a C/SiC cross-weave composite which had been tested in tension to complete fracture is shown in Fig. 17. The

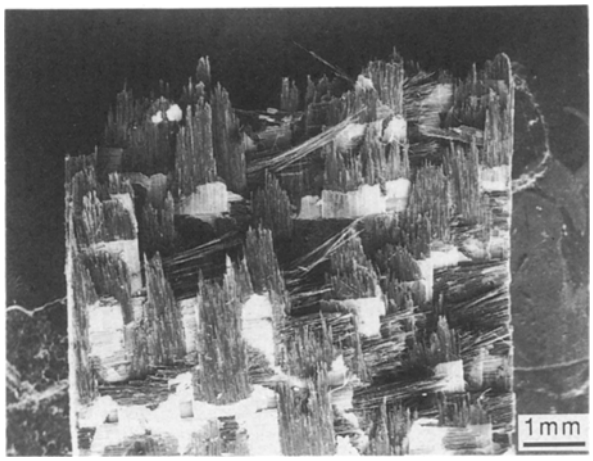

Figure 17 Macroscopic view of the fracture surface of a C/SiC cross-weave composite failed in tension.

fracture surface is characterized by fabric strands failed at various elevations, and extensive pull-out of fibres. Lateral and normal views of the fibre bundle fracture viewed at higher magnifications are shown in Figs 18 and 19, respectively. These show what is considered to be a characteristic feature of the fracture in the composite, namely, protruding groups of ruptured fibres. Essentially, a crack has formed and propagated transversely through a small group of fibres

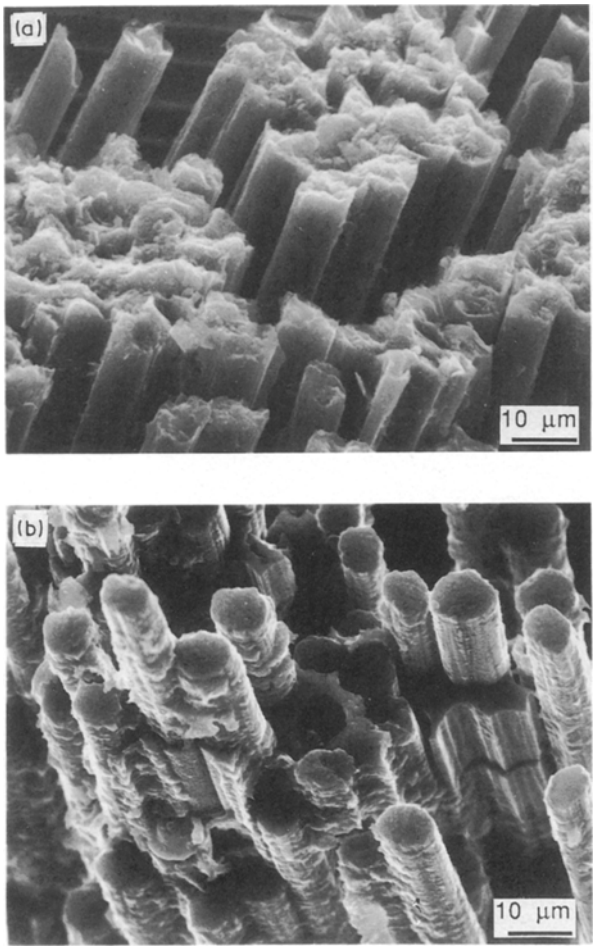

Figure 18 Characteristic feature of fibre bundle fracture viewed at an angle to the fracture surface. (a) Near the sample edge, (b) in the sample interior, showing adherence of the ceramic to the fibres.

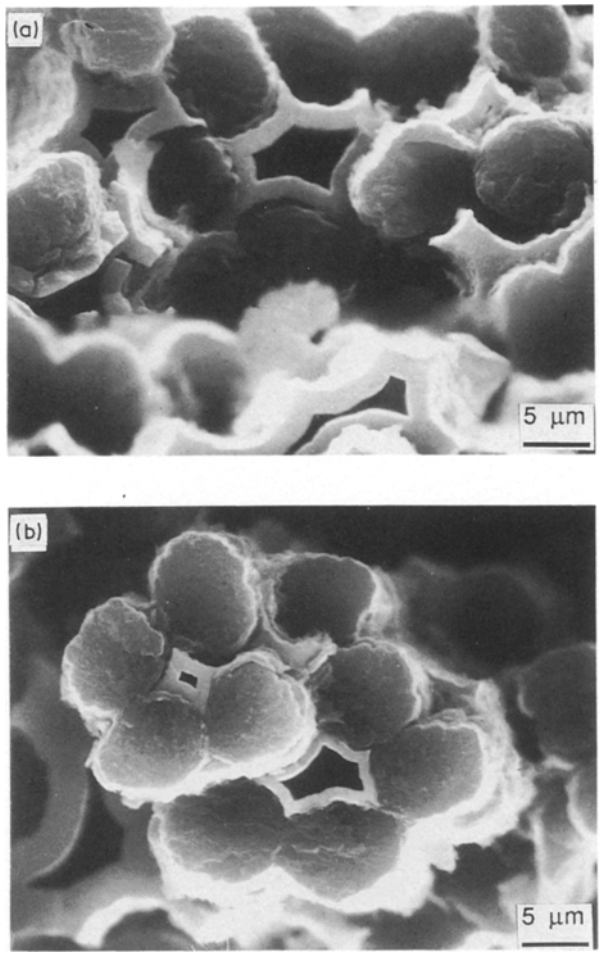

Figure 19 Characteristic features of fibre bundle fracture, viewed normal to the fracture surface.

but then the cracks turn parallel to the specimen axis and produce fracture at the fibre–matrix interface, defining a small cylinder of fractured fibres. This group-linked fracture process is distinct from "fibre pull-out" which generally follows matrix cracking rather than being part of it.

A typical number of fibres involved in this group process is not large, but appears to lie between four and eight. This fractographic evidence demonstrates that the composite does not fail because of one single dominant crack, being bridged by, and then rupturing, the fibres. Such a fracture surface is reminiscent of that of a unidirectional glass fibre/polymer matrix composite but in such a case single fibres protrude from the surface [10]. It is well known that a jagged irregular failure surface is caused by the accumulation of fibre breaks at random places, prior to failure. It therefore stands to reason that the failure surface for the ceramic composites results from a similar accumulation of flaws involving groups of fibres. This has led us to a failure scenario which concludes that transverse cracks are arrested by matrix voids, causing the cracks to grow along the fibres. After they have travelled some distance by fibre–matrix interface fracture, the cracks become stable and arrested. Therefore, fibre debonding and fibre group pull-out are considered to be the two major damage modes in the early stages of the fracture process. Fractographic studies also revealed fibre debonding and pull-out in the final stages

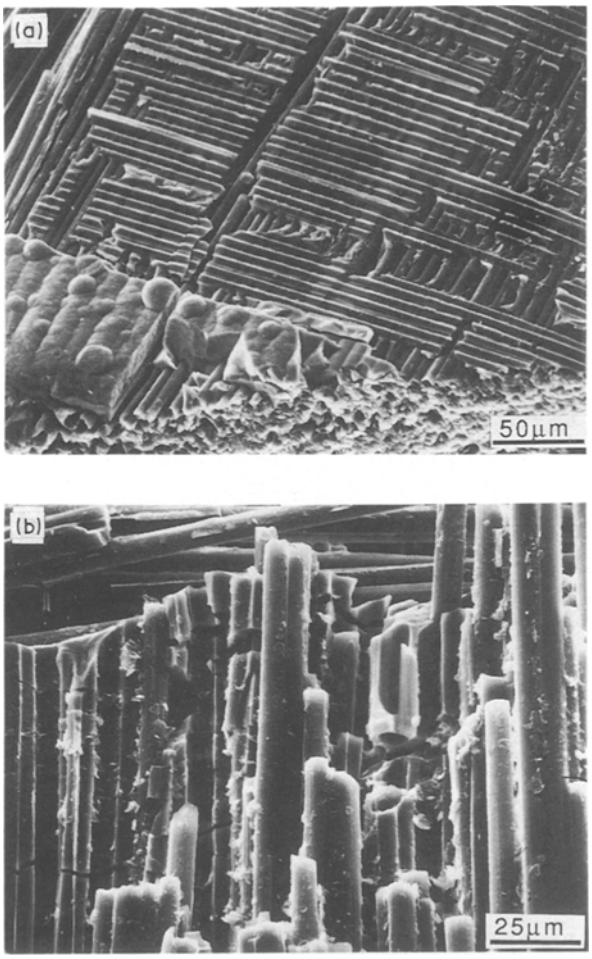

Figure 20 Scanning electron micrographs of fracture surface, showing fibre debonding and pull-out (a, b) and showing an example of a matrix crack cutting fibres (b).

of fracture as shown in Fig. 20. Fig. 20b also provides evidence that matrix cracks sometimes stimulate rupture of the fibres, causing them to be cut in the plane of the matrix crack.

6. Conclusions

Deformation and fracture tests of C/SiC composite, coupled with microstructural observation of the damage, have led to the following summary and conclusions.

1. The C/SiC cross-weave composite studied contains a variety of macro and micro voids: systematic gaps in the interstices of the weave and a variety of cylindrical microvoids within the ceramic-impregnated strands of the carbon-fibre weave. No interfacial layer was found between the fibres and matrix.

2. Specimens have been subjected to mechanical tests both in tension and compression. As expected, the behaviour in tension and compression was found to be asymmetric. The stress–strain curve in tension shows a fairly low elastic limit, followed by a regime of inelastic behaviour with a continuous reduction of stiffness. However, the stress–strain curve in compression and the tensile stress–strain curve of a preloaded specimen mainly show linear elastic behaviour.

3. The initial deviation from linearity in the tensile tests of as-received specimens is caused by the formation of matrix cracks. This microcracking process in the matrix is presumed to be governed by residual stresses. The ultimate failure occurs when such flaws interact and coalesce resulting in fibre bundle failure and pull-out.

4. The failure surface is very irregular in nature and consists of distinct groups of about four to eight ruptured fibres "pulled out" as a group from the matrix. Therefore, the propagation of one dominant crack is not the mode of failure. A possible failure scenario is that local cracks rupture similar fibre groups with transverse cracks which are arrested by the internal voids and then the cracks propagate in the fibre direction by fibre–matrix interface fracture until these cracks become self arrested. Catastrophic failure follows by the linking of these group fractures and ultimately, massive fibre debonding.

Acknowledgements

The research was performed under a contract from the Air Force Office of Scientific Research to the Material Sciences Corporation. Experimental work was supported by a subcontract to the University of Pennsylvania with complementary support from the Benjamin Franklin Program of the State of Pennsylvania and the University. We are grateful to the funding agencies for their support and also to the Laboratory for Research on the Structure of Matter for providing test facilities.

References

1. L. J. SCHILLER and J. J. STIGLICH Jr, *Amer. Ceram. Bull.* **65** (1986) 289.
2. D. B. MARSHALL and J. E. RITTER, *ibid.* **66** (1987) 309.
3. T. MAH, M. G. MENDIRATTA, A. P. KATZ and K. S. MAZDIYASNI, *ibid.* **66** (1987) 304.
4. R. A. J. SAMBELL, D. H. BOWEN and D. C. PHILLIPS, *J. Mater. Sci.* **7** (1973) 663.
5. *Idem., ibid.* **7** (1972) 676.
6. D. B. MARSHALL and A. G. EVANS, *J. Amer. Ceram. Soc.* **68** (1985) 225.
7. T. MAH, M. G. MENDIRATTA, H. P. KATZ, R. RUH and K. S. MAZDIYASNI, *ibid.* **68** (1985) C27–C30.
8. H. S. STARRETT, Southern Research Institute, communicated data (1985).
9. O. SHAIZERO and A. G. EVANS, *J. Amer. Ceram. Soc.* **69** (1986) 481.
10. D. HULL, "An Introduction to Composite Materials" (Cambridge University Press, 1981) Ch. 7.

Received 12 January
and accepted 19 November 1990